Desalination 619 (2026) 119551

Contents lists available at ScienceDirect

Desalination

journal homepage: www.elsevier.com/locate/desal

Novel approaches for valorisation of waste brines at pilot scale via electrodialysis with bipolar membranes

G. Virruso [a,1], C. Cassaro [a,1], A. Tamburini [a,b,*], A. Cipollina [a,b], G. Micale [a,b]

[a] Dipartimento di Ingegneria, Università degli Studi di Palermo, Viale delle scienze Ed. 6, 90128, Palermo, Italy
[b] ResourSEAs S.r.l., Via Notarbartolo n. 38, 90141, Palermo, Italy

HIGHLIGHTS

- Saline feed schemes investigation at pilot scale to improve EDBM's brine treatment capacity.
- Same behaviour was observed by feeding only the acid or base compartment with the brine.
- The innovative Water Salt Backflip (WS-BF) configuration was proposed and tested.
- Similar performance observed between WS-BF and the standard feed and bleed mode at high concentrations.

GRAPHICAL ABSTRACT

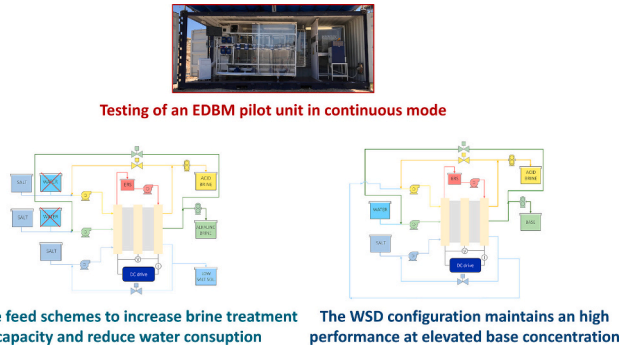

ARTICLE INFO

Keywords:
EDBM
BMED
Water consumption
Continuous operation
Saline feed

ABSTRACT

Minimum Liquid Discharge (MLD) schemes are gaining interest to comply with stricter discharge regulations and to recover useful resources. However, MLD schemes pose new challenges in terms of non-conventional operations in well-established industrial processes. As an example, Electrodialysis with Bipolar Membrane (EDBM), which valorises a saline solution through the production of acids and bases and requires large quantities of water, can be operated by sending a brine into the chemicals compartment instead of water. Thus, increasing the brine treatment capacity and reducing the water consumption of EDBM. The produced chemical solutions present a salt background, but it may become irrelevant for a variety of applications inside and outside MLD schemes. The present work evaluates such novel operating schemes at pilot scale, adopting the feed and bleed configuration. Three different scenarios, in which a brine is provided (i) to the acid compartment, (ii) to the base compartment and (iii) to both of them, were investigated and compared with a reference condition. The results showed a slight reduction in concentration (~15 %) feeding one of the two compartments with the brine, while a more pronounced reduction (~ 30 %) was observed feeding both compartments. This suggests that the environmental benefit is achieved at the cost of a performance reduction. Moreover, an innovative scheme, called Water Salt BackFlip (WS-BF), was proposed and tested. The WS-BF produced a high-purity base product and acid product

* Corresponding author at: Dipartimento di ingegneria, Università degli studi di Palermo, Viale delle scienze Ed. 6, Palermo, 90128, Italy.
E-mail address: alessandro.tamburini@unipa.it (A. Tamburini).
[1] These authors equally contributed to the work.

https://doi.org/10.1016/j.desal.2025.119551
Received 5 August 2025; Received in revised form 23 September 2025; Accepted 23 October 2025
Available online 24 October 2025

with a lower salt content. Improved performance were observed, especially at high base target, in addition to the environmental benefits.

1. Introduction

Currently, many regions in the world are facing major water shortages related to climate change, industrialisation and increasing population [1,2]. A recent report by the *United Nations* claims that over the period 2002–2021, droughts affected over 1.4 billion people, causing severe consequences for the population [3]. About 40 % of the world population lives within 100 km of the coastline [4], suggesting that desalination represents an effective way to tackle this issue.

The desalination process reduces the dissolved salt content of waters present on Earth (i.e., sea, lake, river, etc) to make them potable. Commercially available technologies can be divided into two main categories: thermally driven and membrane-based processes [5]. Multi-stage flash (MSF), multi-effect distillation (MED) and mechanical vapour compression (MVC) are widely adopted thermal desalination technologies. The main advantages of these methods are the high quality of the produced water [6], reliability and longevity [7], as well as the possibility of valorising waste heat sources [8]. As a drawback, there is a considerably high energy consumption in the range of 5–30 kWh kg^{-1} [9] and a high capital investment [10]. The most common membrane-based desalination technologies are: Reverse Osmosis (RO), Electrodialysis (ED) and Membrane Distillation (MD). Among them, RO represents the leading technology, accounting for approximately 90 % of membrane-based desalination plants, thanks to its low energy consumption and water production costs [11]. Membrane-based processes are attractive due to their modularity nature, the reduced investment cost and the relatively low complexity of operation [12]. As disadvantages, membranes must be periodically replaced, and fouling effects can significantly reduce the process performance.

Desalination processes produce a freshwater stream and a highly concentrated solution, known as brine [13]. The disposal of the brine creates some environmental concerns due to its hypersaline content and the presence of chemical compounds, utilised for antifoaming and antiscaling purposes [14]. To tackle this issue, the treatment of the brine has been proposed to reduce the environmental impact by decreasing the discharged volume. This approach is commonly referred as Minimal Liquid Discharge (MLD) or Zero Liquid Discharge (ZLD), depending on the fraction of the initial volume valorised (i.e., approximately lower than and higher than 90 %, respectively) [15]. MLD and ZLD treatment processes aim to recover freshwater along with valuable materials, such as chemicals or minerals, through the adoption of *ad hoc* processes, which commonly operate in series [16]. Among these processes, ElectroDialysis with Bipolar Membranes (EDBM) is gaining attention thanks to the possibility of converting brine into useful acid and base streams [17]. This aspect can be used in two different ways: i) producing chemicals with high purity that can be sold to the industrial sector [18]; ii) internally recirculating the obtained chemicals to other processes of the ZLD/MLD treatment process, with lower purity standards, to recover valuable minerals [19]. In both cases, the presence of EDBM can positively affect the treatment process, selling products or avoiding purchasing them.

The working principle of EDBM foresees the dissociation of water thanks to the bipolar membranes (BMs) and selective passage of ions due to the presence of monopolar ion-exchange membranes (i.e., cation (CEM) and anion (AEM) exchange membranes) [20]. The driving force of the entire process is an electric field, established by adopting a couple of electrodes [21]. Between them, several membranes are packed to increase the process capacity. The repetitive unit of an EDBM process, known as triplet, consists of a CEM, an AEM and BM as well as three solution compartments (i.e., acid, base and salt) obtained by separating the membranes with polymeric spacers [22]. A schematic representation of the EDBM process is depicted in Fig. 1.

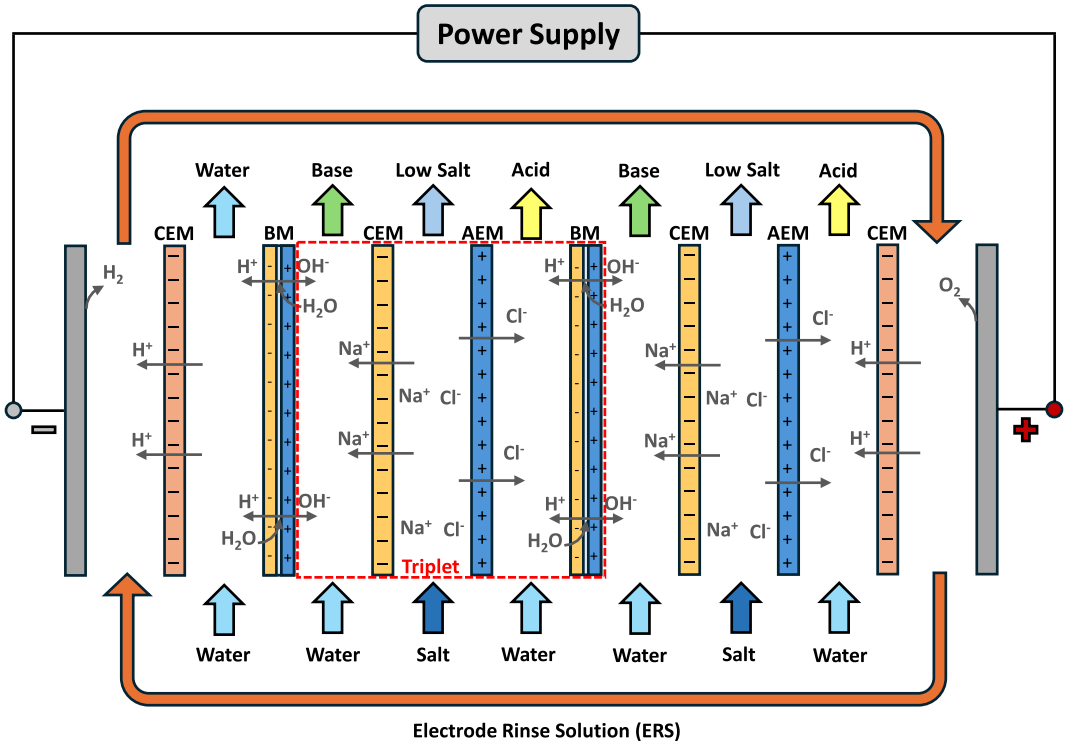

Fig. 1. Working principle of an Electrodialysis with bipolar membranes (EDBM) system.

The EDBM process has been almost exclusively used for chemicals production, by feeding the chemicals compartment with low concentrated acid or base solutions (typically in the range 0.05–0.1 mol L^{-1}) [18,23] or even low conductivity water [24], obtaining purity of acid and base in the range 85–95 % [18]. Thus, suggesting that the chemicals produced by EDBM can be used in those cases in which a salt contamination can be tolerated or should be purified with downstream processes. The possibility of feeding low-concentration acid or base solutions with a salt background in the chemicals compartments was evaluated by Culcasi et al. [25]. The authors experimentally investigated a laboratory-scale EDBM unit (active membrane area of 100 cm^2) in open-loop mode, feeding an acidified brine (i.e., 0.2 mol L^{-1} of HCl and 0.25 mol L^{-1} of NaCl) and an alkaline brine (i.e., 0.2 mol L^{-1} of NaOH and 0.25 mol L^{-1} of NaCl) in the acid and base compartments, respectively. An almost constant applied voltage was observed for the current density range 20–250 A m^{-2}, while no experimental information is available about the performance of the process. Recently, Filingeri et al. [26] evaluated the effect of feeding a higher concentrated salt background (i.e., 2 mol L^{-1} of NaCl) in addition to low concentrated acid and base solutions (i.e., 0.05 mol L^{-1} of HCl or NaOH) to the chemical compartments of EDBM. The authors tested two laboratory-scale EDBM units (provided from Fumatech (Germany) and SUEZ (France), with an active membrane area of 100 and 280 cm^2, respectively) in closed-loop configuration. Interestingly, the authors compared the performance of feeding one chemical compartment at a time and both simultaneously with a reference condition, in which there was no salt background in the chemical compartments. The results revealed that introducing the brine only into the base compartment led to similar performance compared to the reference scenario, while feeding the acid compartment or both chemical compartments led to a performance reduction of the base product in the range 9–20 % and 40–70 %, respectively.

Based on the previous literature, the objective of the present work is to study the innovative EDBM schemes proposed by Filingeri et al. [26] at pilot scale, adopting a continuous operating mode (i.e., feed and bleed), which appears the most promising for the EDBM scale-up, thanks to its good performance at high current densities [27]. A brine with a concentration similar to that produced by a seawater RO units (i.e., 1 mol L^{-1} of NaCl) [23] was tested, as it is the most abundant in the desalination field. A wide range of operating conditions was assessed by changing current density, chemicals and salt flowrates. Additionally, an innovative process configuration, called Water Salt – BackFlip (WS-BF), was proposed, tested and compared with the innovative schemes, to prove that a much better performance can be reached, similar to the standard EDBM scheme, mitigating the effect of salt background presence.

2. Materials and methods

2.1. Experimental set-up

This study was carried out using an EDBM pilot plant, which was realised within the framework of the Horizon 2020 Water-Mining project, as part of the demonstrative treatment chain Case Study 1 [28]. The EDBM pilot plant is a containerised unit and consists of a pumping station and a stack unit.

The pumping station houses all the instrumentation needed to monitor and control the main process variables. Specifically, magnetic induction flowmeters (OPTIFLUX 4100C, KROHNE Messtechnik GmbH), pH sensors (SMARTPAT PH 8320, KROHNE Messtechnik GmbH), pressure transducers (OPTIBAR P 1010C, KROHNE Messtechnik GmbH) and conductivity sensors (OPTISENS IND 1000, KROHNE) are installed to monitor flowrates, pH values, pressures as well as conductivities and temperatures, respectively. As control elements, magnetic-driven centrifugal pumps with a regenerative turbine (PTM 2.5 × 6, made in PP, TEOREMA S.r.l.), electrically actuated valves (VKDIV/CE DN15, made in PP, FIP – Formatura Iniezione Polimeri S.p.A.) and gear pumps (FG200–300 with 4 mm gears, made in AISI 316 L, TEOREMA S.r.l.) are used to control inlet, recirculated and outlet flowrates, respectively.

The stack unit is composed of the EDBM stack and the DC power supply. This unit is electrically isolated from the pumping station to guarantee operator safety by means of PVC vertical panels. The EDBM stack is an FT-ED1600–3 unit, purchased from FuMA-Tech GmbH (Germany). A total of 40 triplets, divided into two cell packs of 20 triplets each, are installed, enabling the unit to reach a total active membrane area of 19.2 m^2, which is one of the biggest reported in the literature so far [27]. The cell packs are hydraulically connected in series, while they are electrically powered in parallel. Two different cathodes, made in stainless steel, are located at both ends of the unit, whereas a shared anode (i.e., DSA®) is centred between the two cell packs. In the cell packs, FUMASEP® FAB, FUMASEP® FKB, and FUMASEP® FBM (Germany) are employed as anion, cation and bipolar membranes, respectively. Polypropylene woven spacers with a thickness of 350 μm thick are installed. The DC drive (GIUSSANI S.r.l.) is able to power the EDBM stack up to 200 A or 80 V.

The pilot plant was also equipped with a total number of six HDPE IBC tanks with a volume 1 m^3 each, for acid, base and salty solution, while a PE cylindrical tank of 0.125 m^3 was employed for the electrode rinse solution (ERS).

Further details about the EDBM pilot plant can be found in previous works [27,29].

2.2. Solution preparation and analytical procedures

The brine fed to EDBM's compartments was prepared by mixing NaCl grains (>99.5 % purity, Saline di Volterra S.r.l) with seawater Reverse Osmosis (RO) permeate (i.e., ~ 350 μS cm^{-1}), reaching a concentration of 1 mol L^{-1} NaCl. For the electrode rinse solution (ERS) compartment, a 0.25 mol L^{-1} solution of Na_2SO_4 was employed, dissolving high-purity powder (technical grade, CR GRUPO CRIMIDESA) into RO permeate. During tests, solution conductivities, flowrates, temperatures, pH values and inlet pressures as well as current and voltage supplied to the stack, were continuously recorded, with a frequency of 1 Hz. Acid and base samples (50 mL) were collected once per hour for the analytical characterisation. Titrations were manually performed using Na_2CO_3 (0.05 mol L^{-1}) and HCl (0.1 mol L^{-1}), for the acid and base solutions, respectively, using methyl orange as indicator.

2.3. EDBM process configuration for brine valorisation

2.3.1. Saline feed schemes in feed and bleed mode

Several process configurations are available for EDBM's applications, both continuous and discontinuous. Between them, the feed and bleed process configuration appears attractive thanks to its performance, the wide range of produced chemical concentrations and the different control strategies that can be adopted [30]. The feed and bleed configuration partially recirculates the outlet solutions of acid, base and salt to the corresponding stack inlet. In this way, water can be provided as inlet stream to the acid and base compartments, avoiding an elevated stack resistance. A schematic representation of the feed and bleed configuration is shown in Fig. 2a.

Novel operating layouts were explored as variations of the conventional feed and bleed configuration, which differ for the stream fed to the chemical compartments (i.e., a brine instead of water). The brine feed is denoted with an "S", meaning saline (i.e., brine) feed, to obtain the acronym of the saline feed schemes, while the water feed is indicated with a "W". The adopted sequence of feeding solutions to name each scheme is acid, base and salt. Specifically, three different schemes, in which the brine is fed to the acid (i.e., SWS scheme) or to the base compartment (i.e., WSS scheme) or to both chemical compartments (i.e., SSS scheme), were investigated and compared with the conventional feed and bleed configuration or Water Water Salt (WWS) layout. Table 1

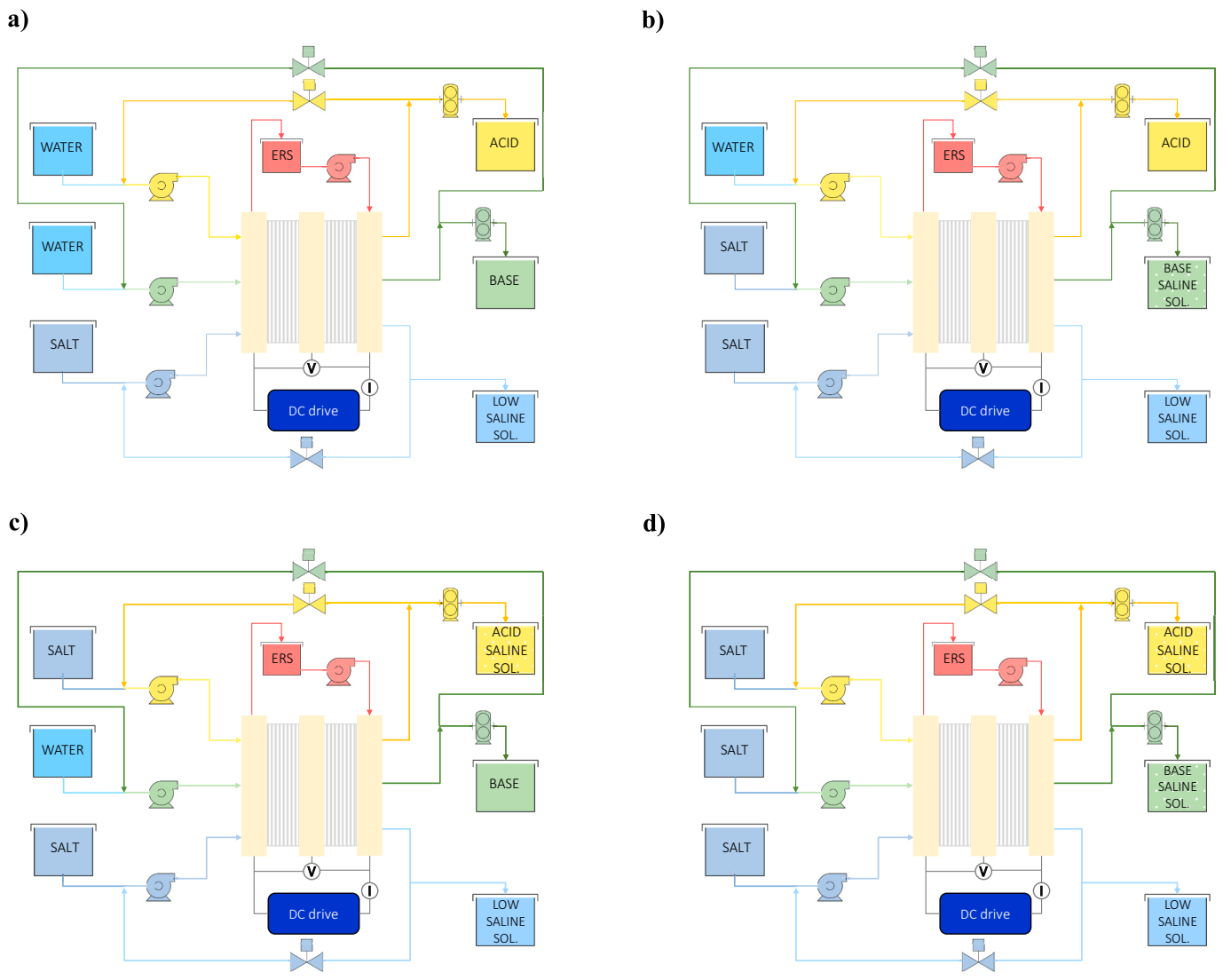

Fig. 2. Tested schemes adopting the feed and bleed mode: a) standard feed and bleed mode or Water-Water-Salt (WWS) scheme; b) Water-Salt-Salt (WSS) scheme; c) Salt-Water-Salt (SWS) scheme; d) Salt-Salt-Salt (SSS) scheme. The adopted sequence of feeding solutions to name each scheme is acid, base and salt.

Table 1
Details of the feeding solution for the investigated layouts in feed and bleed mode.

Scheme	Acid feed	Base feed	Salt feed
WWS	Water	Water	Salt sol.
WSS	Water	Salt sol.	Salt sol.
SWS	Salt sol.	Water	Salt sol.
SSS	Salt sol.	Salt sol.	Salt sol.

summarises the feeding solution for the saline feed schemes and for the standard feed and bleed configuration.

The WWS scheme foresees feeding the salt solution only into the salt compartment, while the acid and base compartments are fed with water. In this layout, the main solutions exit from the EDBM are a low-concentrated saline solution from the saline compartment as well as acid and base solutions from their respective compartments. Generally, high-purity acid and base solutions are produced with a low salt content, which depends on its transfer from the saline to the acid and base channels due to diffusion, internal leakage, non-perfectly permselectivity of membranes and other undesired phenomena occurring within the stack.

In the WSS scheme, shown in Fig. 2b, the base compartment, in addition to the salt compartment, is fed with the salt solution, while the acid channel is supplied with water. In this case, the produced chemical solutions are an acid solution with low salt contamination and an alkaline saline solution, with a salt concentration similar to the inlet one. The SWS scheme (Fig. 2c) is analogous to the WSS scheme. Indeed, the salt solution is fed into the acid compartments, while water is provided to the base compartment. The produced solutions are a high-purity base solution and an acidified salt solution with reduced purity. In the SSS scenario (Fig. 2d) all the compartments, except for the electrode compartment, are supplied with the salt solution. In this case, the obtained solutions are an acid and an alkaline saline solutions. The latter scheme almost completely eliminates the water consumption of the EDBM process (except for the water needed to prepare the ERS), while, at the same time, the volume of treated brine is approximately three times larger. In the schemes WSS and SWS the water consumption is almost halved, while the brine treatment capacity of the EDBM system is almost doubled.

2.3.2. *The Water Salt BackFlip configuration*

A novel process configuration is here described as a variation of the saline feed schemes: it is named Water Salt BackFlip (WS-BF) configuration, as it utilises only two streams as inputs: water (W) and a saline solution (S) in the base and salt compartment, respectively, while the

acid compartment is feed with the outlet salt solution from the salt compartment, which is directed back to the acid inlet (BF). A schematic representation of the WS-BF configuration is shown in (Fig. 3) Due to the direct connection between the outlet of the salt compartment and the inlet of the acid one, the circulating flowrate is almost constant, except for the water flux between membranes. The outlet saline solution from the salt compartment has already been depleted of most of its dissolved salts to produce chemicals, prior to entering the acid compartment. This offers a significant advantage compared to the standard saline feed schemes in which the acid compartment is fed with the inlet brine (i.e., SWS and SSS). Although it is similar to the SWS scheme in terms of water consumption reduction, an improvement in the quality of the acid product is obtained due to the reduced salt content. Additionally, recirculating the outlet salt solution within the unit eliminates the need for downstream treatment processes. Finally, this configuration prevents the loss of produced acid that would normally occur during standard operation. As a matter of fact, due to the high mobility of the protons, they pass through the AEM, reaching the salt compartment. The outlet solution obtained from the salt compartment is here fed to the acid one, which positively affects its overall performance, since it already contains protons at the entrance of the acid compartment.

2.4. Description of the test conducted

All the schemes were tested in different operating conditions to evaluate their performance. Specifically, four steady-state conditions were assessed for each scheme in a wide range of current densities (i.e., 200–400 A m^{-2}), chemical flowrates (i.e., 0.5–2 L min^{-1}) and salt solution flowrates (i.e., 0.75–1.5 L min^{-1}). Table 2 illustrates the investigated steady-state conditions.

These operating conditions were selected to: i) test the pilot under a typically adopted current density range [31]; ii) to produce products with a concentration approximately in the range 0.5–1 mol L^{-1}, iii) to study the effect of current density on the process performance.

At fixed current density of 400 A m^{-2}, an outlet salt flowrate of 1.5 L min^{-1} (steady-state A and B) was used, while at 200 A m^{-2}, a halved outlet salt flowrate (steady-state C and D) was set to maintain a similar concentration gradient in the salt compartment. It can be noted that the steady-state conditions at the two different current densities are perfectly proportional in terms of outlet flowrates. For instance, when the current density is doubled, the outlet flowrates also double (steady-state A is proportional to C, while B is proportional to D). Each scheme

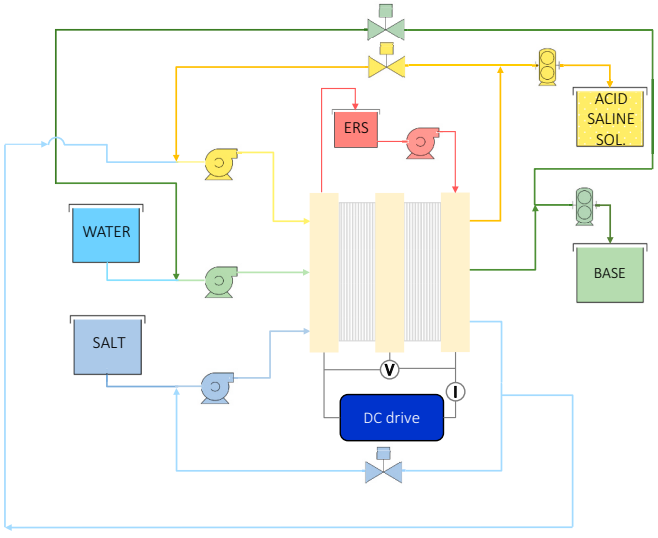

Fig. 3. Schematic representation of the Water Salt BackFlip (WS-BF) configuration. The EDBM unit produces two output streams: a base stream with high purity and an acid solution with a reduced salt concentration.

Table 2
Operative conditions investigated with the EDBM pilot plant for each scheme.

Steady-state	i (A m^{-2})	$Q_{a,out}$* (L min^{-1}))	$Q_{b,out}$ (L min^{-1}))	$Q_{s,out}$ (L min^{-1})
A	400	2	2	1.5
B	400	1	1	1.5
C	200	1	1	0.75
D	200	0.5	0.5	0.75

* For the WS-BF configuration, the outlet acid flowrate ($Q_{a,out}$) is almost equal to the outlet salt flowrate ($Q_{s,out}$), except for the osmotic/electro-osmotic effects.

was investigated in a single test in which the four operating conditions were evaluated. For each steady-state condition, three samples were collected and analysed. The average results from the three samples were used to compare the schemes. The ERS compartment was always operated at a constant flowrate of 20 L min^{-1}. Results reproducibility was assessed by repeating several operating conditions. A good reproducibility, in the range 5–20 % was observed and error bars are included to all the experiments presented in the manuscript.

2.5. Performance indicators

The following performance indicators are adopted in this study to evaluate the characterise the system.

Current efficiency (CE), also known as current utilisation, represents the fraction of supplied electric charges successfully converted into acid and base products.

$$CE = \frac{\left(Q_{p,out}\, C_{p,out} - Q_{p,in}\, C_{p,in}\right)F}{60\, N_{tr}\, i\, A_m}\ [\%] \tag{1}$$

where $C_{p,in}$ and $C_{p,out}$ refer to the inlet and outlet concentration (mol L^{-1}) of product p (i.e., either NaOH or HCl) to/from the system, respectively, $Q_{p,in}$ and $Q_{p,out}$ represent solution inlet and outlet flowrates (L min^{-1}) of p, F is Faraday's constant (i.e., 96,485C mol^{-1}), N_{tr} is the triplet number, A_m is the active membrane area (m^2) and i (A m^{-2}) is the current density supplied to the unit.

Specific Energy Consumption (SEC) indicates the energy consumed to produce 1 kg of the desired product (i.e., either NaOH or HCl).

$$SEC = \frac{U\, i\, A_m}{60\left(Q_{p,out}\, C_{p,out} - Q_{p,in}\, C_{p,in}\right) M_p}\ \left[kWh\, kg^{-1}\right] \tag{2}$$

in which U is the potential difference (V) applied to the stack, and M_p is the molar mass of the desired product (g mol^{-1}).

Specific Productivity (SP) provides the mass of product p produced in a working year (8000 h) per unit of total membrane area.

$$SP = \frac{60 \bullet 8,000}{10^6}\, \frac{Q_{p,out}\, C_{p,out} - Q_{p,in} C_{p,in}}{3\, A_m\, N_{tr}} M_p\ \left[ton\, y^{-1} m^{-2}\right] \tag{3}$$

Since the acid and base compartments were supplied with RO permeate, the initial concentration of product p, $C_{p,out}$, was considered negligible.

Water Footprint (WFP) quantifies the consumed water to produce 1 kg of product p (i.e., either NaOH or HCl).

$$WFP = \frac{Q_{p,in}}{\left(Q_{p,out}\, C_{p,out} - Q_{p,in} C_{p,in}\right) M_p 10^{-3}}\ \left[L\, kg^{-1}\right] \tag{4}$$

where all the variables have the meaning described above.

3. Results and discussion

3.1. Standard and saline feed operating schemes in feed and bleed

3.1.1. Standard feed and bleed mode (WWS): Reference scheme

The performance of the EDBM unit was firstly assessed by adopting

the standard feed and bleed configuration, in which water is provided into the chemical compartments. This scheme is indicated as Water Water Salt (WWS). Fig. 4 shows the result obtained with the WWS scheme. For steady-state condition A, depicted as filled squares, concentration values slightly higher than 0.5 mol L^{-1} were obtained for both chemicals, with values of 0.53 and 0.57 mol L^{-1} for acid and base, respectively (Fig. 4a). Halving the chemical flowrates at fixed current density of 400 A m^{-2}, the steady-state condition B, indicated with filled circles, was reached, with values of acid and base concentrations below 1 mol L^{-1}. This suggests that a current efficiency reduction was obtained from steady-state A to B due to the higher impact of non-ideal phenomena (such as diffusion, parasitic currents, etc.) at higher concentrations. The base concentration reached a value of 0.88 mol L^{-1}, which is significantly higher than the corresponding acid concentration of 0.76 mol L^{-1}. This can be attributed to the higher diffusion of protons into the saline channels, producing a pH reduction of the latter and, at the same time, decreasing the number of moles available in the acid compartment. Adjusting the current density from 400 to 200 A m^{-2} and halving the salt flowrate value brings to steady-state condition C, represented with empty rhombus. In this case, concentration values of 0.49 and 0.54 mol L^{-1} were registered for acid and base, respectively. These concentration values were slightly lower compared to those obtained in steady-state A. Finally, steady-state D was explored halving acid and base flowrates at a constant current density of 200 A m^{-2} and at a salt

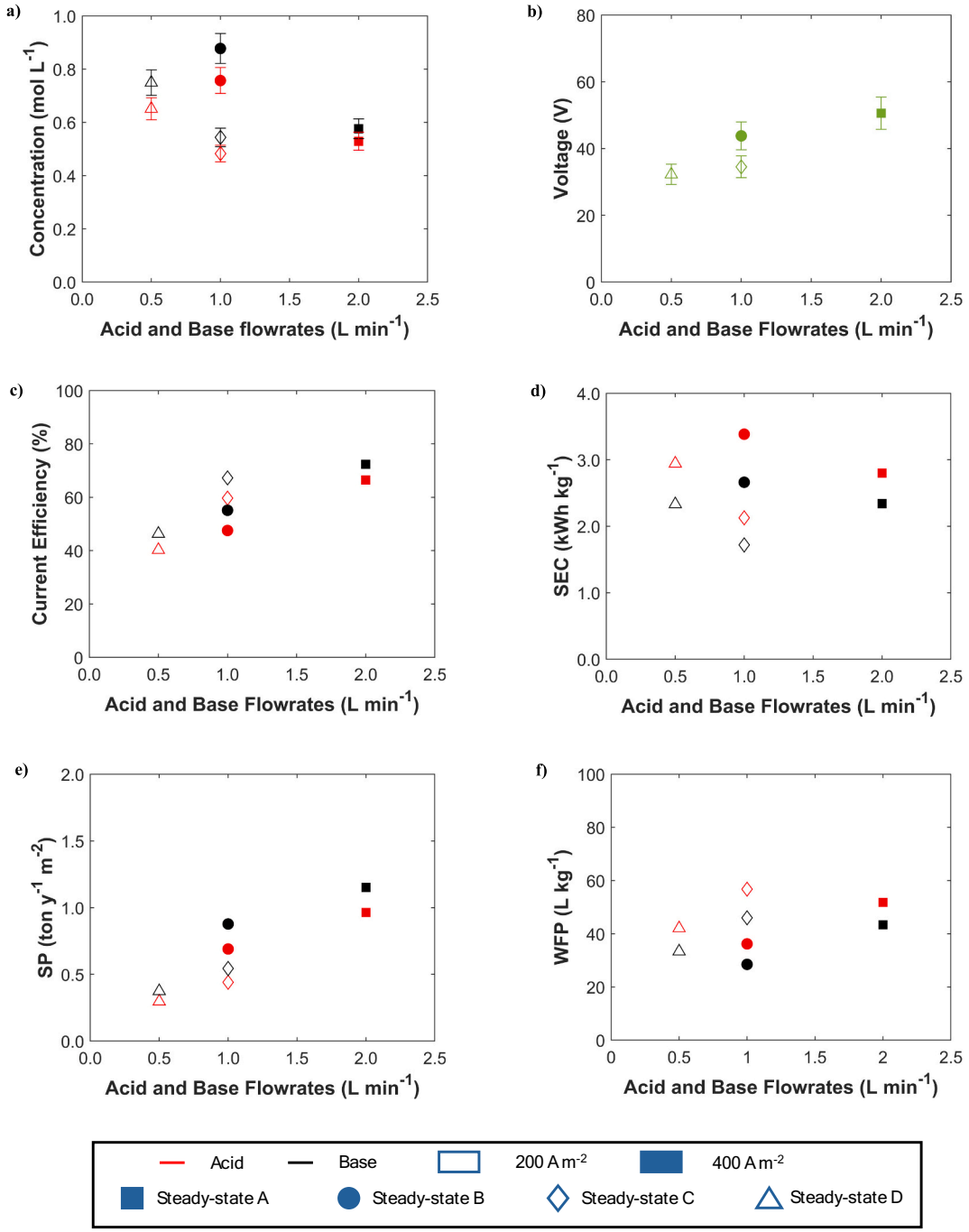

Fig. 4. Main results obtained with WWS scheme (i.e., standard feed and bleed mode): a) acid and base concentrations in terms of protons and hydroxide ions; b) external voltage applied to the stack; c) current efficiency; d) specific energy consumption; e) specific productivity; f) water footprint. The x-axis denoted with "Acid and Base flowrates (L min^{-1})" refers to the fact that the two chemicals flowrates were maintained equal to each other.

flowrate of 0.75 L min^{-1}, indicated with empty triangles. This resulted in significantly lower concentrations compared to the corresponding steady state at 400 A m^{-2} (i.e., steady state B). This can likely be explained by an increased influence of the diffusive flux compared to the migrative one, due to the lower current density.

The trend of the external voltage is shown in Fig. 4b. In steady-state A a value of about 50 V was reached. Moving to steady-state B, a reduction in external voltage was observed, reaching 44 V, which can be attributed to the decrease in stack resistance due to the increased concentration of both acidic and basic solutions. Halving the current density, in the last two steady-states the voltage reached values of about 35 V and 32 V, for steady-state C and D, respectively. Considering the CE, shown in Fig. 4c, the highest value where registered for steady-state A, with values of 66 % and 72 % for acid and base, respectively. Reducing the value of chemical flowrates, leads to lower values of 48 % and 55 % for acid and base, respectively. Considering the steady-states at lower current density, their CE values resulted significantly lower compared to the corresponding value at 400 A m^{-2}. In detail, reductions between 7 % and 9 % were observed passing from steady-state A to C, while more pronounced reductions were observed moving from steady-state B to D, in the range 17–33 %, with a higher value for the acid product. Regarding the SEC, shown in Fig. 4d, values of 2.3 and 2.8 kWh kg^{-1} were obtained for base and acid in steady state A. In steady state B, an increase in SEC was observed due to the sharp reduction in CE, which decreases more than the external voltage. The lowest values of SEC were obtained in steady-state C, with values of 2.1 and 1.7 kWh kg^{-1} for acid and base, respectively. In steady-state D, values slightly lower compared to those found for steady-state B were observed, despite the significant voltage reduction. The trends of SP can be seen in Fig. 4e. The highest values were obtained in steady-state condition A for both chemicals, equal to 0.96 and 1.2 ton y^{-1} m^{-2} for acid and base, respectively. It can be seen that the SP gradually decreased passing from steady-state A to D, reaching the minimum values of 0.3 and 0.37 ton y^{-1} m^{-2} in the last steady-state for acid and base, respectively. In Fig. 4f the water footprint is shown. Values of acid and base WFP equal to 52 and 43 L kg^{-1} were obtained, respectively, in steady-state A. A reduction in WFP is observed in steady-state B compared to A, due to the increase in product concentrations. Specifically, values of 36 and 28 L kg^{-1} for acid and base, respectively. Halving the current density leads to an increase in the WFP, between 6 % and 17 %, compared to the corresponding steady-states at 400 A m^{-2}. This increase is related to the reduction of the product concentrations at lower current densities, which in turn depends on the CE reduction (Fig. 4c).

3.1.2. *Feeding one chemical compartment with a brine: WSS and SWS schemes*

Following the reference scenario, two mirrored schemes were investigated, the one with the saline solution fed into the base

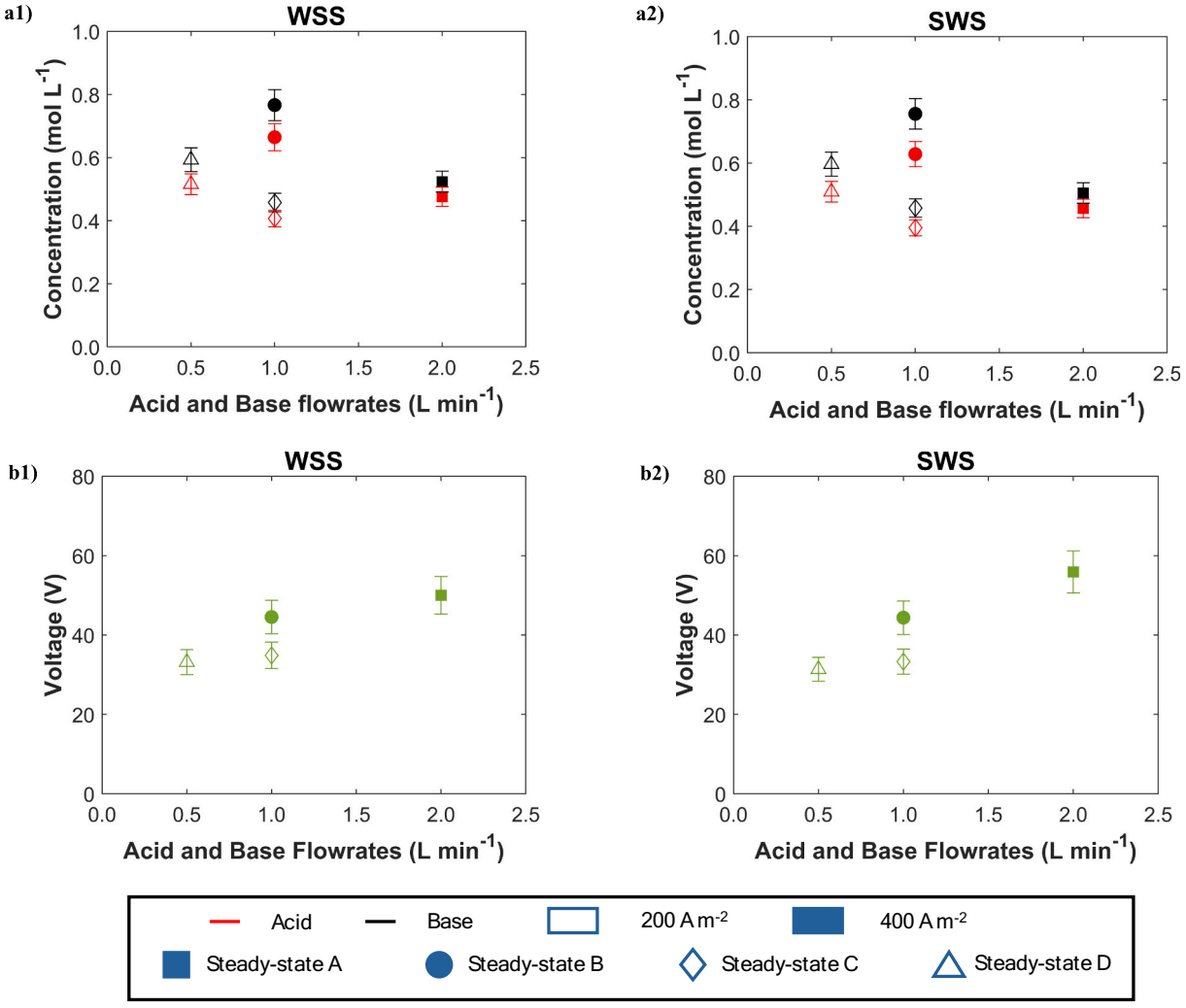

Fig. 5. Acid and base concentrations values in terms of protons and hydroxide ions concentrations for: a1) WSS scheme and a2) SWS scheme; external applied voltage values for: b1) WSS scheme and b2) SWS scheme. The x-axis denoted with "Acid and Base flowrates (L min^{-1})" refers to the fact that the two chemicals flowrates were maintained equal to each other.

compartment and the other with the saline solution fed into the acid compartment, referred to as WSS and SWS schemes, respectively. The concentration and voltage trends for these two scenarios are shown in Fig. 5. The concentration of acid and base reported in this paragraph refers to their protons and hydroxide ions concentrations, respectively.

As it can be seen from Fig. 5, concentration and voltage trends are very similar for the two specular schemes. In the WSS scheme, although the base channel is fed with the saline solution, concentrations of 0.52 mol L^{-1} for the base and 0.48 mol L^{-1} for the acid product were achieved in steady-state A (Fig. 5a1). Feeding the saline solution into the acid compartment (i.e., SWS scheme), the results remained almost unchanged, with an output concentration of 0.51 mol L^{-1} for the base and a concentration of 0.46 mol L^{-1} for the acid (Fig. 5a2). In steady-state B, adopting the WSS scheme, a slightly higher acid concentration of 0.66 mol L^{-1} was achieved compared to the SWS scheme (i.e., 0.63 mol L^{-1}), whilst for the base product, similar alkaline concentrations were reached (i.e., approximately 0.75 mol L^{-1}). In the steady-state C, almost the same concentrations of acid and base were obtained between the two schemes, with values of 0.41 and 0.47 mol L^{-1} for acid and base, respectively. In steady-state D concentrations below 0.6 mol L^{-1} for both chemicals were observed.

Considering the external voltage trends of the stack (Fig. 5b1 and b2), it can be observed that the SWS reached a slightly higher voltage value (approximately 10 %) than the WSS scheme, which lies within the experimental error. Instead, similar voltage values of approximately 44 V were obtained in steady-state B. Finally, lowering the current density leads to slightly lower values for the SWS scheme. Indeed, in steady-state C and D voltage values of about 35 V and 33 V were obtained for the WSS scheme, while for the SWS scheme values of 33 and 31 were achieved, respectively. Considering the performance parameters for schemes WSS and SWS, the trends resulted qualitatively similar to the reference scenario, as shown in Fig. 6. Nevertheless, slight differences were observed between SWS and WSS schemes due to the different effects of the brine in the acid and base compartments, respectively.

In steady-state A, similar CE values were obtained between the WSS and SWS schemes (Fig. 6a1 and a2), for both acid and base. Specifically, CE values in the range 63–65 % for the base product and 57–60 % for the acid were found, with higher values registered for the WSS scheme. In steady-state B, fairly low CE values (below 50 %) were obtained for both chemicals, with the acid CE dropping down to 42 % (WSS scheme) and 40 % (SWS scheme), while for the base a value of 48 % was obtained in both schemes. In steady-state C, values of CE of approximately 57 % for the base and 50 % for the acid were obtained for the two schemes. Finally, in steady-state D, CE dropped below 40 % for both products, with the two schemes leading to similar values of 32 % and 37 % for acid and base, respectively. The trends of the SEC are shown in Fig. 6b1 and b2 and, as observed for the CE, very similar values were obtained between the two schemes. Higher SEC values of approximately 16 % were observed in steady-state A for the SWS scheme due to the higher external voltage values (SEC is directly proportional to the external voltage, Eq. (2)), with values of 3.6 kWh Kg^{-1} and 2.9 kWh Kg^{-1} for acid and base, respectively. Maximum SEC values of were observed in steady-state B, with SEC values of about 4.0 kWh Kg^{-1} and 3.1 kWh Kg^{-1} for acid and base, respectively, for both schemes. Significantly lower SEC values were observed in steady-state C due to the lower current density and concentration reached, with values of approximately 2.5 kWh Kg^{-1} and 2 kWh Kg^{-1} for acid and base, respectively, for both schemes. In steady-state D the SWS scheme lead to slight lower SEC, with values of 3.6 kWh Kg^{-1} and 2.9 kWh Kg^{-1} for acid and base, respectively In terms of SP, almost overlapped values were obtained (Fig. 6c1 and c2). Maximum SP values equal to 0.9 ton y^{-1} m^{-2} and 1 ton y^{-1} m^{-2} were observed for acid and base, respectively, in steady state *A. minimum* values of 0.2 ton y^{-1} m^{-2} and 0.3 tons y^{-1} m^{-1} were, on the other hand, registered in steady-state D for acid and base, respectively. The values of WFP for the two mirrored scheme are shown in Fig. 6d1 and d2. Specifically, values of WFP equal to zero were obtained for the base and acid product for WSS and SWS scheme, respectively, in all the investigated steady-states. Indeed, the use of a brine in one of the chemicals compartments produces a nought WFP of the corresponding product. For the WSS scheme, values of WFP of the acid product in the range 44–69 m^3 kg^{-1} were obtained, with higher values for low current densities and reduced concentrations. For the SWS scheme, WFP between 33 and 55 m^3 kg^{-1} for the base product were reached, with the lowest value obtained in steady-state B (i.e., higher concentration and higher current density). The larger WFP values of the acid product are related to the lower concentration reached compared to the base product and to lower molecular weight.

Ultimately, the two mirrored schemes appear to have an almost identical behaviour as a function of the operative conditions. Few differences were observed in the voltage values, approximately 10 % of difference in steady-state A, that can be related to the stack resistance, which in turn depends on the membranes and solution resistances and on the electromotive force, although it is close to the experimental error. This suggests that the presence of a brine in one of the two channels next to the BM has the same effect on the process, leading to similar product concentration and performance. Thus, the selection of one of these two schemes depends mainly on product requirements, to be used inside or outside the MLD treatment chain.

3.1.3. *Feeding both chemicals compartments with a brine: SSS scheme*

This section presents the results of the SSS scheme, in which the brine was fed into the acid, base and salt compartments. Fig. 7 shows the results of the test carried out. In steady-state A, a base concentration of 0.45 mol L^{-1} and an acid concentration of 0.41 mol L^{-1} were achieved (Fig. 7a). In steady-state B, a slight increase in the concentrations was observed, with values of 0.52 and 0.63 mol L^{-1} for acid and base, respectively. In the other two steady states at 200 A m^{-2} (i.e., steady-state C and D), quite low concentration values were observed. In detail, in steady-state C, values barely above 0.3 mol L^{-1} were reached for both acid and base, while in the last steady-state D values of 0.35 and 0.43 mol L^{-1} for acid and base were found, respectively. Looking at the external voltage (Fig. 7b) voltage values between 33 and 50 V were obtained in the investigated steady-states. The obtained values were comparable with those obtained in the WWS scheme (Fig. 4b), suggesting that the presence of salt did not significantly affect the resistance of the stack.

Considering the performance indicator, it can be observed from Fig. 7c, values of CE higher than 60 % were never achieved for both chemicals. In addition, extremely low current efficiency values were obtained in steady-state D, with values of 21 and 26 % for acid and base, respectively. The current efficiency severely affects the specific energy consumption, with values of the latter up to 5.6 kWh kg^{-1} in steady-state D. From Fig. 7d, it can be observed that there is a significant difference between the SEC of acid and base in all the steady states investigated. The results highlight how, in this case, the effect of current efficiency prevailed over that of voltage in determining the specific consumption. Indeed, while the voltage remained close to 33 V in the steady-states at 200 A m^{-2}, the CE was extremely low, leading to a significant increase in the consumption. The values of SEC in steady-state D resulted higher than the corresponding steady-state at 400 A m^{-2}, for both chemicals, despite of the halved current density and the consequent reduction of the voltage drop. The collapse in the current efficiency also impacted the specific productivity. In steady-state A, SP values lower than 1 ton y^{-1} m^{-2} were reached for both chemicals. The SP values decreased over the steady-states (from A to D), reaching a specific productivity of around 0.2 ton y^{-1} m^{-1} for both acid and base in steady state D. Finally, WFP values of zero were obtained for both products in the investigated steady-states, due to the use of brine as inlet stream of the chemicals compartments. These results suggest that the environmental benefits in terms of consumed water are reached at a cost of a process performance reduction, with a reduction in concentration of approximately 30 % compared to the WWS scheme.

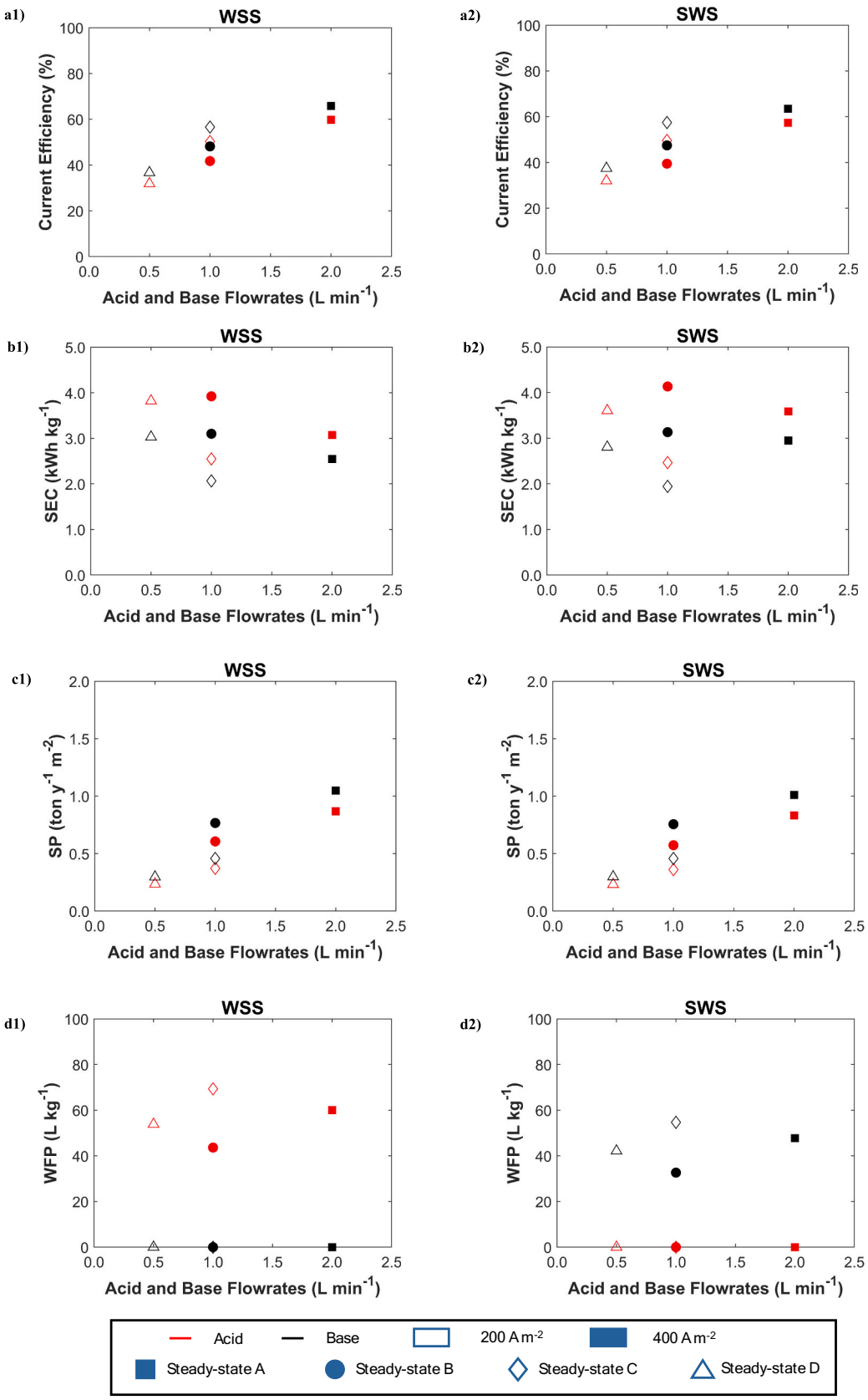

Fig. 6. Representative values of acid and base performance indicators for WSS and SWS schemes: a1) current efficiency for WSS scheme, a2) current efficiency for SWS scheme, b1) specific energy consumption for WSS scheme, b2) specific energy consumption for SWS scheme, c1) specific productivity for WSS scheme, c2) specific productivity for SWS scheme; d1) water footprint for WSS scheme, d2) water footprint for SWS scheme. The x-axis denoted with "Acid and Base flowrates (L min^{-1})" refers to the fact that the two chemicals flowrates were maintained equal to each other.

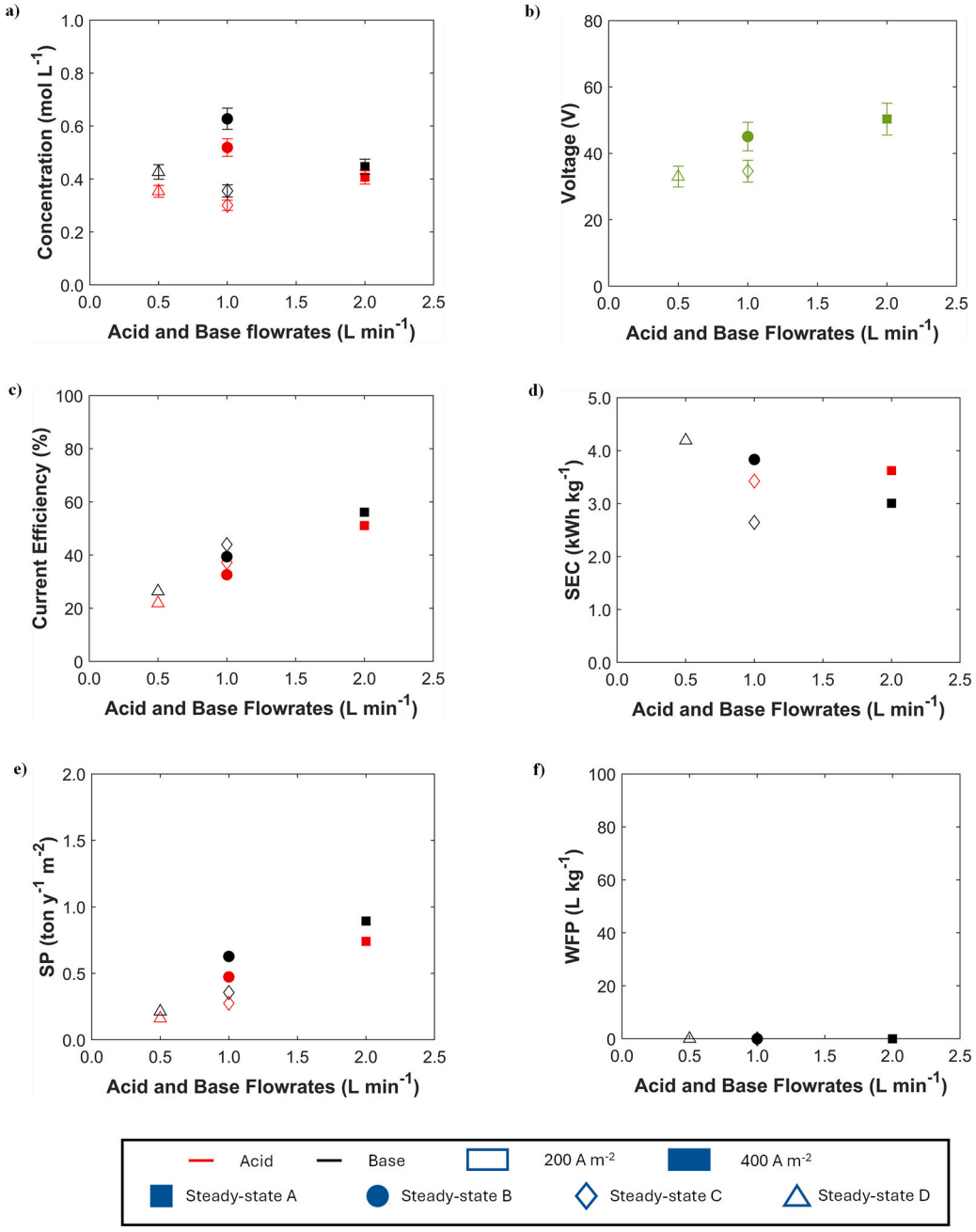

Fig. 7. Main results obtained with the SSS scheme: a) acid and base concentrations in terms of protons and hydroxide ions; b) external voltage applied to the stack; c) current efficiency; d) specific energy consumption; e) specific productivity, f) water footprint. The x-axis denoted with "Acid and Base flowrates (L min^{-1})" refers to the fact that the two chemicals flowrates were maintained equal to each other.

3.2. Water Salt BackFlip (WS-BF) configuration

The WS-BF process configuration was evaluated by adopting the same operating conditions utilised for schemes operated in feed and bleed mode. Here, the value of the acid flowrate was set equal to the salt flow rate due to their direct connection (see Table 2). Fig. 8 shows the results related to the WS-BF configuration.

In the first evaluated steady-state (i.e., steady-state A), a current density of 400 A m^{-2} as well as an acid (equal to the salt) and base flowrate of 1.5 and 2.0 L min^{-1}, respectively, were used. An acid product concentration of 0.6 mol L^{-1} was achieved, higher than the base concentration, equal to 0.5 mol L^{-1} (Fig. 8a). Reducing the base flowrate to 1.0 L min^{-1} at fixed current density and acid flowrate (i.e., steady-state B) produced a significant increase in base product concentration, reaching more than 0.9 mol L^{-1}, at an almost fixed acid concentration (i.e., 0.6 mol L^{-1}). In general, lower acid concentrations enable to reach higher base concentrations as the two solutions interact, due to (i) diffusive effects and (ii) non-perfect selectivity of the membranes In the steady-state C, a current density of 200 A m^{-2} along with acid and base flowrate of 0.75 and 1 L min^{-1}, respectively, were employed. The concentrations reached in this case were 0.54 and 0.46 mol L^{-1} for the acid and base, respectively. In steady-state D, only the base flowrate was changed with respect to the third steady-state, to a value of 0.5 L min^{-1}. The acid concentration remained practically unchanged, while the base concentration reached a value of approximately 0.7 mol L^{-1}.

External voltage values in the range 31–44 V (Fig. 8b) were obtained, which resulted slightly lower compared to the standard feed and bleed mode, especially at higher current density.

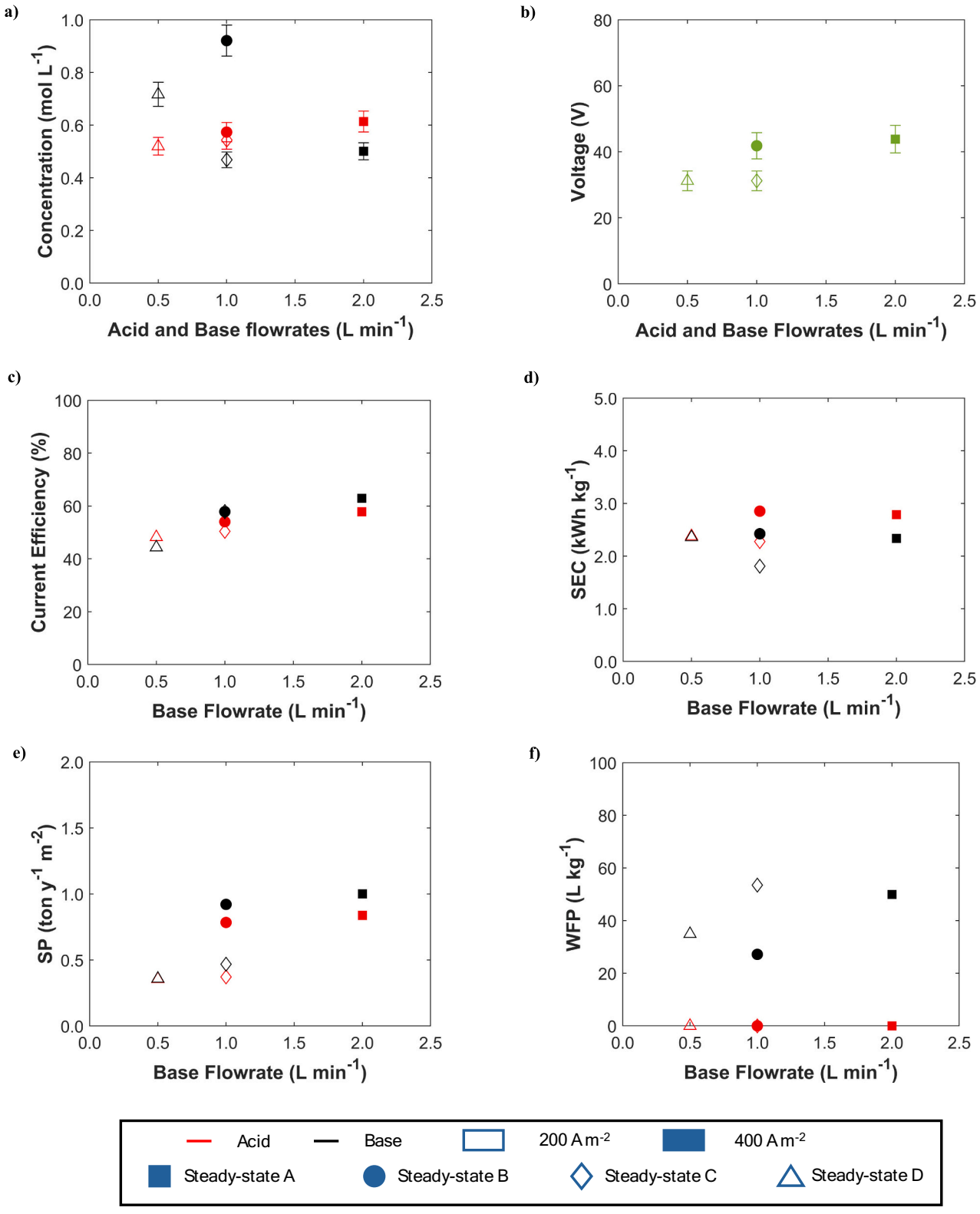

Fig. 8. Main results obtained with the WS-BF process configuration: a) acid and base concentrations in terms of protons and hydroxide ions; b) external voltage applied to the stack; c) current efficiency; d) specific energy consumption; e) specific productivity; f) water foot-print.

Current efficiency values between 44 and 63 % were observed for the base product in the investigated steady-states (Fig. 8c), while for the acid product values between 48 and 58 % were reached. SEC values in the range 1.8–2.4 kWh kg^{-1} were found (Fig. 8d), which resulted quite low considering the concentration reached and the current density utilised. Specific productivity up to 1.1 ton y^{-1} m^{-2} was also registered in the last investigated steady-state (Fig. 8e). WFP values equal to zero were obtained for the acid product, whereas for the base product values

in the range 27–54 $m^3\ kg^{-1}$ were obtained. In steady-state B, the lowest WFP value was reached due to the high base product concentration (i.e., 0.92 mol L^{-1}).

3.3. Comparison

This paragraph provides a comprehensive comparison of all the investigated schemes and process configuration focusing on the product of greatest interest, sodium hydroxide. Fig. 9a presents bar charts showing the concentrations obtained in all the investigated steady-states. A reduction was obtained in the hydroxide ions concentration passing from the WWS scheme, i.e., standard feed and bleed configuration, to the saline feed schemes. It could be noted that WSS and SWS schemes led to the same concentration values in all the investigated steady-states. This means that the presence of a brine in one of the compartments adjacent to the bipolar membrane leads to the same performance. An increase in the salt-limiting current density is expected due to the presence of salt in one of the chemicals compartment adjacent to the BM, which lead to a higher diffusive flux of salt from the compartment toward the interlayer, thus reducing the water-splitting capability of the membrane [32]. In the SSS scheme, this effect is exacerbated because both the adjacent compartments of the bipolar membrane contain a high salt concentration, thus there will be two higher diffusive fluxes toward the interlayer of the BM. Indeed, comparing the different steady-states, more marked concentration reductions (compared to the WWS scheme) were observed at low current density (i.e., steady states C and D). Specifically, percentual reductions in the range 16–35 % and 21–43 % were registered in steady-states C and D, respectively. Considering the WS-BF configuration, similar base concentrations to those reached in WSS and SWS schemes were obtained for steady-states A and C, in which a lower chemicals concentrations were reached. Interestingly, at higher alkaline product concentrations (i.e., steady-state B and C), the WS-BF configuration shows a meaningful performance enhancement, with values of concentration perfectly comparable with the REF scheme or slightly better. The reason for this could be attributed to the lower acid concentration in the acid

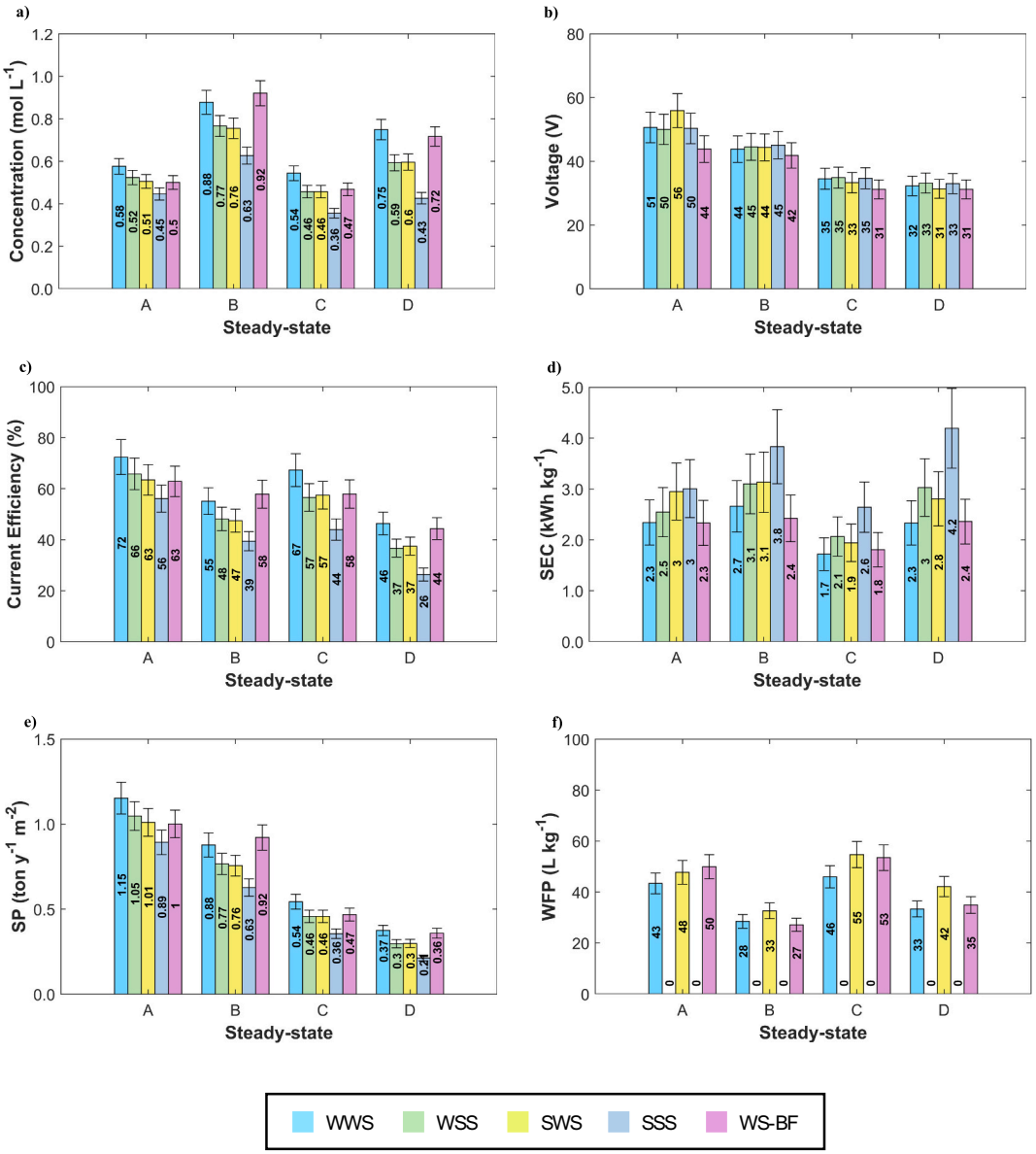

Fig. 9. Comparison between the standard feed and bleed scheme (WWS) and the three saline feed schemes and the innovative WS-BF configuration in terms of: a) hydroxide ion concentration of the base product, b) external applied voltage to the stack, c) current efficiency, d) specific energy consumption; e) specific production and f) water footprint of the base product.

compartment due to the higher acid flowrate (almost equal to salt flowrate) which leads to a reduction of undesired detrimental phenomena (e.g. diffusive fluxes).

Comparing the applied voltage values to stack between the different schemes and stack configuration (Fig. 9b), almost constant values were observed. The saline feed schemes show almost the same voltage values compared to the WWS, while for the WS-BF a slightly lower values were observed at lower products concentrations (i.e., steady-states A and C). This effect could be related to the acid product which reached slightly higher concentration compared to the other schemes (i.e., 0.61 and 0.54 mol L^{-1} in WDS, for steady-state A and C, respectively, as well as in the ranges 0.41–0.53 mol L^{-1} and 0.30 and 0.48 mol L^{-1}) and to the direct connection with the salt compartment.

In Fig. 9c the current efficiency values are reported. As expected, the CE decreases as the concentration rises and this effect was observed both at 400 A m^{-2} (steady-states A and B) and 200 A m^{-2} (steady-states C and d). What is worthy of note is that the current efficiency is higher at higher currents. In fact, comparing steady-states A with C as well as B with D (which are proportional to each other in terms of operating conditions) an increase in the current efficiency was observed for the investigated schemes at higher current densities (Fig. 9c). This results in an interesting characteristic of the feed and bleed mode [27,33] and it was observed for all the investigated schemes and configuration.

The specific energy consumption depends on the CE because the voltage remains almost unchanged between the schemes (Fig. 9b). An opposite trend with respect to CE was observed with the lowest values reached in steady-state C (Fig. 9d), thanks to the high current efficiency along with the lower voltage values related to the current density adopted (i.e., 200 A m^{-2}). Whilst the highest values were observed in steady-state B except for SSS scheme, for which a more substantial consumption was registered in steady-state D, due to the quite low value of the current efficiency. For the WS-BF configuration, the same value of SEC was obtained in steady-states B and D. In terms of specific productivity, significantly higher values were obtained in steady-state A for all the schemes, with values between 0.9 and 1.2 ton y^{-1} m^{-2}, Fig. 9e. It is interesting to note that the WS-BF shows the largest SP in steady-state, also higher than the WWS. This is related to the higher base concentration, which was reach also thanks to lower acid product concentration.

In terms of WFP of the base product, WSS and SSS lead to values equal to zero, while, between the other schemes, the WWS has the lowest values in almost all the steady-states, Fig. 9f. The WS-BF produces lightly higher values than WWS in steady-states A and C, while for the other steady- states comparable values were obtained.

These results highlight that feeding the acid and base channels with saline solution (i.e., saline feed schemes) leads to a gradual decline in performance as well as in the maximum achievable concentration. However, they allowed for the identification of operating conditions where there is no significant drop in performance (i.e., high current densities and low chemicals concentrations), which could be considered when implementing innovative layouts for EDBM to reduce water consumption and improve the brine treatment capacity. In this regard, the operating condition identified as preferable, in terms of performance parameters, is steady-state A, independently of the scheme adopted, thus confirming what has already been obtained in previous studies [27,33].

These results also proved the attractiveness of this innovative WS-BF process configuration, which allows for maintaining similar performance compared to the WWS condition, at higher chemicals concentrations, despite the feed of the outlet salt stream into the acid compartment. Thus, enabling to reduce the water consumption, and the associated costs, as well as increasing the brine treatment capacity of the process, with no appreciable decline in the performance. This configuration should be preferred if higher base concentrations than 0.5 mol $L^{-1}$are required, while for lower base concentrations around 0.5 mol L^{-1} it results comparable with the corresponding saline feed scheme (i.e., SWS).

4. Conclusions and future outlooks

Novel schemes for brine valorisation, adopting the feed and bleed configuration, were tested to reduce water consumption and improve the brine treatment capacity of the process. The results indicate that feeding a brine in one of the chemical compartments, leads to performance reduction between 9 and 14 % in terms of concentration, at 400 A m^{-2}, for the base production. While a significant lower performance was observed when feeding the brine in both chemical compartments, with reduction up to 44 %. The adoption of these schemes should be economically evaluated considering water cost reduction, for example, in drought areas in which water is produced from seawater, and the environmental benefits obtained from a larger volume of treated brine. An innovative process configuration, indicated as WS-BF, was proposed and tested for the first time. A remarkable improvement in performance was observed with respect to the non-conventional schemes, reaching comparable or even slightly better performance than the conventional feed and bleed configuration at high target concentrations. This process configuration should be preferred in all the fields in which acid brines could be tolerated, such as in the desalination compartment and water treatment, thanks to the beneficial water reduction while maintaining similar performance with the standard feed and bleed mode. Future research will economically assess these innovative schemes, especially the WS-BF, in a wider range of operating conditions, to guide their selection in different scenarios. Moreover, a mirrored scheme of the WS-BF, in which the direct connection is between the outlet salt compartment and the inlet base one, will be tested and compared with the WS-BF reported in this work.

CRediT authorship contribution statement

G. Virruso: Writing – original draft, Visualization, Methodology, Investigation. **C. Cassaro:** Writing – original draft, Visualization, Methodology, Investigation. **A. Tamburini:** Writing – review & editing, Validation, Supervision, Project administration, Methodology, Funding acquisition, Conceptualization. **A. Cipollina:** Writing – original draft, Validation, Project administration, Methodology, Funding acquisition, Conceptualization. **G. Micale:** Writing – review & editing, Validation, Project administration, Methodology, Funding acquisition, Conceptualization.

Declaration of competing interest

The authors declare that they have no known competing financial interests or personal relationships that could have appeared to influence the work reported in this paper.

Acknowledgments

This project has received funding from the European Union's Horizon 2020 - Research and Innovation Framework Programme under Grant Agreement no. 869474 (WATER-MINING-next generation water-smart management systems: large scale demonstrations for a circular economy and society). www.watermining.eu

Data availability

Data will be made available on request.

References

[1] M.M. Mekonnen, A.Y. Hoekstra, Sustainability: four billion people facing severe water scarcity, Sci. Adv. 2 (2016), https://doi.org/10.1126/sciadv.1500323.
[2] M. Mannan, M. Alhaj, A.N. Mabrouk, S.G. Al-Ghamdi, Examining the life-cycle environmental impacts of desalination: a case study in the State of Qatar, Desalination 452 (2019) 238–246, https://doi.org/10.1016/j.desal.2018.11.017.

[3] Water for prosperity and peace, United Nations Educational, Scientific and Cultural Organization, 2024.
[4] M. Ayaz, M.A. Namazi, M.A.U. Din, M.I.M. Ershath, A. Mansour, E.-H.M. Aggoune, Sustainable seawater desalination: current status, environmental implications and future expectations, Desalination 540 (2022), https://doi.org/10.1016/j.desal.2022.116022.
[5] C. Fritzmann, J. Löwenberg, T. Wintgens, T. Melin, State-of-the-art of reverse osmosis desalination, Desalination 216 (2007) 1–76, https://doi.org/10.1016/j.desal.2006.12.009.
[6] G. Scelfo, A. Trezzi, F. Vassallo, A. Cipollina, V. Landi, C. Xenogianni, A. Tamburini, D. Xevgenos, G. Micale, Demonstration of ultra-high-water recovery and brine concentration in a prototype evaporation unit: towards zero liquid discharge desalination, Sep. Purif. Technol. 354 (2025), https://doi.org/10.1016/j.seppur.2024.129427.
[7] A. Cipollina, G. Micale, L. Rizzuti, A critical assessment of desalination operations in Sicily, Desalination 182 (2005) 1–12, https://doi.org/10.1016/j.desal.2005.03.004.
[8] A. Liponi, C. Wieland, A. Baccioli, Multi-effect distillation plants for small-scale seawater desalination: thermodynamic and economic improvement, Energy Convers. Manag. 205 (2020), https://doi.org/10.1016/j.enconman.2019.112337.
[9] A. Alkaisi, R. Mossad, A. Sharifian-Barforoush, A review of the water desalination systems integrated with renewable energy, Energy Procedia (2017) 268–274, https://doi.org/10.1016/j.egypro.2017.03.138.
[10] G. Cipolletta, N. Lancioni, Ç. Akyol, A.L. Eusebi, F. Fatone, Brine treatment technologies towards minimum/zero liquid discharge and resource recovery: state of the art and techno-economic assessment, J. Environ. Manage. 300 (2021), https://doi.org/10.1016/j.jenvman.2021.113681.
[11] Z.M. Ghazi, S.W.F. Rizvi, W.M. Shahid, A.M. Abdulhameed, H. Saleem, S.J. Zaidi, An overview of water desalination systems integrated with renewable energy sources, Desalination 542 (2022), https://doi.org/10.1016/j.desal.2022.116063.
[12] R.W. Baker, Membrane Technology and Applications, Second, Wiley, London, 2012, https://doi.org/10.1002/9781118359686.
[13] A. Panagopoulos, K.-J. Haralambous, M. Loizidou, Desalination brine disposal methods and treatment technologies - a review, Sci. Total Environ. 693 (2019), https://doi.org/10.1016/j.scitotenv.2019.07.351.
[14] A. Shokri, M. Sanavi Fard, A comprehensive overview of environmental footprints of water desalination and alleviation strategies, Int. J. Environ. Sci. Technol. 20 (2023) 2347–2374, https://doi.org/10.1007/s13762-022-04532-x.
[15] A. Panagopoulos, K.-J. Haralambous, Minimal Liquid Discharge (MLD) and Zero Liquid Discharge (ZLD) strategies for wastewater management and resource recovery-Analysis, challenges and prospects, J. Environ. Chem. Eng. 8 (2020), https://doi.org/10.1016/j.jece.2020.104418.
[16] A. Panagopoulos, V. Giannika, Comparative techno-economic and environmental analysis of minimal liquid discharge (MLD) and zero liquid discharge (ZLD) desalination systems for seawater brine treatment and valorization, Sustain Energy Technol Assess 53 (2022), https://doi.org/10.1016/j.seta.2022.102477.
[17] R. Pärnamäe, S. Mareev, V. Nikonenko, S. Melnikov, N. Sheldeshov, V. Zabolotskii, H.V.M. Hamelers, M. Tedesco, Bipolar membranes: a review on principles, latest developments, and applications, J. Membr. Sci. 617 (2021), https://doi.org/10.1016/j.memsci.2020.118538.
[18] W. Zhang, M. Miao, J. Pan, A. Sotto, J. Shen, C. Gao, B. Van Der Bruggen, Process economic evaluation of resource valorization of seawater concentrate by membrane technology, ACS Sustain. Chem. Eng. 5 (2017) 5820–5830, https://doi.org/10.1021/acssuschemeng.7b00555.
[19] C. Morgante, F. Vassallo, C. Cassaro, G. Virruso, D. Diamantidou, N. Van Linden, A. Trezzi, C. Xenogianni, R. Ktori, M. Rodriguez, G. Micale, D. Xevgenos, Pioneering minimum liquid discharge desalination: a pilot study in Lampedusa Island, Desalination 581 (2024), https://doi.org/10.1016/j.desal.2024.117562.
[20] X. Tongwen, Electrodialysis processes with bipolar membranes (EDBM) in environmental protection - a review, Resour. Conserv. Recycl. 37 (2002), https://doi.org/10.1016/S0921-3449(02)00032-0.
[21] Y. Yang, X. Gao, A. Fan, L. Fu, C. Gao, An innovative beneficial reuse of seawater concentrate using bipolar membrane electrodialysis, J. Memb. Sci. 449 (2014) 119–126, https://doi.org/10.1016/j.memsci.2013.07.066.
[22] H. Strathmann, Ion-Exchange Membrane Separation Processes, First edit, Elsevier B.V., 2004.
[23] M. Reig, S. Casas, O. Gibert, C. Valderrama, J.L. Cortina, Integration of nanofiltration and bipolar electrodialysis for valorization of seawater desalination brines: production of drinking and waste water treatment chemicals, Desalination 382 (2016) 13–20, https://doi.org/10.1016/j.desal.2015.12.013.
[24] Y. Sun, Y. Wang, Z. Peng, Y. Liu, Treatment of high salinity sulfanilic acid wastewater by bipolar membrane electrodialysis, Sep. Purif. Technol. 281 (2022), https://doi.org/10.1016/j.seppur.2021.119842.
[25] A. Culcasi, L. Gurreri, A. Cipollina, A. Tamburini, G. Micale, A comprehensive multi-scale model for bipolar membrane electrodialysis (BMED), Chem. Eng. J. 437 (2022) 135317, https://doi.org/10.1016/J.CEJ.2022.135317.
[26] A. Filingeri, M. Herrero-Gonzalez, J. O'Sullivan, J.L. Rodriguez, A. Culcasi, A. Tamburini, A. Cipollina, R. Ibañez, M.C. Ferrari, J.L. Cortina, G. Micale, Acid/base production via bipolar membrane electrodialysis: brine feed streams to reduce fresh water consumption, Ind. Eng. Chem. Res. 63 (2024) 3198–3210, https://doi.org/10.1021/acs.iecr.3c03553.
[27] C. Cassaro, G. Virruso, A. Culcasi, A. Cipollina, A. Tamburini, G. Micale, Electrodialysis with bipolar membranes for the sustainable production of chemicals from seawater brines at pilot plant scale, ACS Sustain. Chem. Eng. 11 (2023) 2989–3000, https://doi.org/10.1021/acssuschemeng.2c06636.
[28] European Commission, Grant Agreement number- N° 869474 -WATER-MINING, 2020, https://doi.org/10.3030/869474.
[29] G. Virruso, C. Cassaro, A. Culcasi, A. Cipollina, A. Tamburini, I.D.L. Bogle, G.D.M. Micale, Multi-scale modelling of an electrodialysis with bipolar membranes pilot plant and economic evaluation of its potential, Desalination 583 (2024) 117724, https://doi.org/10.1016/j.desal.2024.117724.
[30] G. Virruso, C. Cassaro, F. Vassallo, A. Filingeri, A. Pellegrino, A. Tamburini, A. Cipollina, G.D.M. Micale, A pilot plant investigation on a real seawater brine valorisation via electrodialysis with bipolar membranes, J Water Process Eng 69 (2025) 106741, https://doi.org/10.1016/J.JWPE.2024.106741.
[31] G.P. Thiel, A. Kumar, A. Gómez-González, J.H. Lienhard, Utilization of desalination brine for sodium hydroxide production: technologies, engineering principles, recovery limits, and future directions, ACS Sustain. Chem. Eng. 5 (2017) 11147–11162, https://doi.org/10.1021/acssuschemeng.7b02276.
[32] H. Strathmann, J.J. Krol, H.-J. Rapp, G. Eigenberger, Limiting current density and water dissociation in bipolar membranes, J. Memb. Sci. 125 (1997) 123–142, https://doi.org/10.1016/S0376-7388(96)00185-8.
[33] G. Virruso, C. Cassaro, A. Tamburini, A. Cipollina, G.D.M. Micale, Performance evaluation of an electrodialysis with bipolar membranes pilot plant operated in feed & bleed mode, Chem. Eng. Trans. 105 (2023) 73–78, https://doi.org/10.3303/CET23105013.